Reflection high-energy electron diffraction and photoemission study of GaSb(100) reconstructions

M. T. Sieger, T. Miller, and T.-C. Chiang
Department of Physics, University of Illinois at Urbana-Champaign, 1110 West Green Street, Urbana, Illinois 61801-3080
and Materials Research Laboratory, University of Illinois at Urbana-Champaign,
104 South Goodwin Avenue, Urbana, Illinois 61801-2902
(Received 17 March 1995)

The clean GaSb(100) surface exhibits a variety of reconstructions, including a $c(2\times10)$, a $c(2\times6)$, and a $(1\times3)/c(2\times6)$, in order of a decreasing surface Sb/Ga ratio. Core-level photoemission spectroscopy and reflection high-energy electron diffraction were employed to study each of these reconstructions in detail. Our results show that the $c(2\times6)$ and $(1\times3)/c(2\times6)$ surfaces have significantly different stoichiometries and core-level line shapes, and are, in fact, different reconstructions, rather than variations of the same $c(2\times6)$ surface due to disorder. Analysis of the photoemission data taken with a wide range of incident photon energy suggests that the $c(2\times10)$ surface is very Sb rich, with more than 2 ML of Sb, while the $c(2\times6)$ has $1-\frac{2}{3}$ ML of Sb, and the $(1\times3)/c(2\times6)$ has about $1-\frac{2}{3}$ ML of Sb with $\frac{1}{3}$ ML of Ga atoms intermixed on the surface. Quantum-mechanical diffraction and interference effects are found to significantly affect the measurement of surface-to-bulk photoemission intensity ratios. Surface structure models are presented for each reconstruction which are consistent with the observed data.

I. INTRODUCTION

Much effort has been directed in recent years towards understanding the structure of III-V semiconductor surfaces. Most of this attention has been focused on the GaAs(100) surface, due to its technological significance. However, the other III-V compounds, such as InAs, GaP, and GaSb are often used in device fabrication, most importantly in heterojunction lasers and infrared detectors. It is, therefore, desirable to understand the surface structure of these materials on their own merit as well as for comparison with the GaAs surface. Also, detailed studies of these surfaces are necessary if we hope to eventually develop a unified understanding of compound semiconductor reconstructions. In this paper, we use reflection high-energy electron diffraction (RHEED) and synchrotron radiation photoemission spectroscopy to study GaSb(100) reconstructions.

Previous studies of the GaSb(100) surface have shown the existence of several surface symmetries, including a $c(2\times10)$, a $c(2\times6)$, and a $(1\times3)/c(2\times6)$ in order of decreasing surface Sb concentration.[1-3] For brevity and to avoid semantic confusion with the $c(2\times6)$, we will refer to the $(1\times3)/c(2\times6)$ surface as a (1×3), although there definitely are weak $\frac{1}{2}$ order features in the RHEED pattern. Franklin *et al.*[1] studied the (1×3) surface in some detail and suggested a structural model with $\frac{2}{3}$ ML of Sb and $\frac{1}{3}$ ML of Ga atoms on top of a full ML of Sb. Most studies to date have made no distinction between the $c(2\times6)$ and (1×3) surfaces, assuming that they are the same reconstruction with varying degress of disorder. We show here that the $c(2\times6)$ and (1×3) are structurally similar, but the (1×3) has $\frac{1}{3}$ ML of surface Ga atoms, whereas the $c(2\times6)$ has none. The evolution of the Sb $4d$ core level with annealing temperature shows three distinct regions corresponding to the three reconstructions, and demonstrates conclusively that the $c(2\times6)$ and (1×3) are different reconstructions. The $c(2\times10)$ surface has not been studied with any other method of surface science beyond RHEED, and no structural models have been proposed for this surface to date. We present here the first photoemission study of this reconstruction, and find it to be extremely Sb rich.

Our photoemission measurements of the Ga $3d$ and Sb $4d$ core-level line shapes show surface-shifted components. The relative intensities of these surface-derived features are used to deduce information about the surface structure. In addition, the intensity ratios between the Ga and Sb core levels are used to deduce a measure of the surface stoichiometry. As is well known, core-level spectroscopy is surface sensitive, due to a fairly short photoelectron escape depth, generally in the range of 4–10 Å. In the past core-level intensities were often analyzed in terms of the classical layer attenuation model, with the photoelectron escape depth as the only parameter in the model, and data were typically taken with one (or just a few) photon energy. However, a recent study of the Si(111)-(7×7) $2p$ core level over a wide photon energy range has shown that quantum-mechanical effects caused by photoelectron interference or diffraction are important;[4] as a result, the measured intensity shows significant extended-photoemission fine-structure (EPFS) oscillations that cannot be explained by the smooth "universal curve"[5] of the escape depth as assumed in previous studies. In view of this result on Si(111)-(7×7), our measurement of GaSb employs a wide range of incident photon energy, and significant EPFS intensity oscillations are also found, suggesting that such oscillations may be a general feature of photoemission for all surfaces. The data show that if an intensity analysis is carried out at just one arbitrarily chosen photon energy (as was typically done in the past), the answer can be quite different if the chosen energy happens to be near a maximum or

0163-1829/95/52(11)/8256(10)/$06.00

minimum of the EPFS oscillations. Thus, in our analysis of the intensity data, the classical layer attenuation model is used to describe the average intensity variation only, with the superimposed oscillations ignored. This procedure provides a better measure of the surface stoichiometry.

II. EXPERIMENT

The photoemission experiments were performed at the Synchrotron Radiation Center of the University of Wisconsin-Madison on the 1-GeV storage ring Aladdin. Synchrotron radiation was dispersed by a monochromator, and a Leybold EA-10/100 hemispherical analyzer was used to detect the photoelectrons. Binding energies were referenced to the Fermi level measured from a Cu foil in electrical contact with the sample. Fermi-level spectra indicated an overall system resolution of 0.17 eV for the full width at half maximum. The experiment chamber had a base pressure of 8×10^{-11} torr.

The *n*-type, Te-doped, GaSb(100) wafer with a carrier density of $1.5\times10^{17}/\text{cm}^3$ was purchased from MCP Electronic Materials (England). The polished samples were introduced via a load-lock system to the photoemission chamber, and were outgassed for several hours at 380 °C. Two cycles of sputtering with 500-eV Ar^+ ions (current at sample ~4 μA) and annealing at 500 °C were sufficient to produce a (1×3) RHEED pattern, which was used as a starting surface for molecular-beam epitaxial (MBE) growth. MBE of the GaSb sample surfaces was performed *in situ*. Five-nine pure Ga and Sb were evaporated from electron-beam heated crucibles, with the evaporation rate monitored by a water-cooled quartz crystal thickness monitor. The GaSb growth rate was set to be about 2 ML/min, with 1 ML defined as 5.38×10^{14} atoms/cm^2, which is the site density for the ideally terminated GaSb(100) surface. The GaSb(100) substrate was heated by passing a current directly through the sample, and the substrate was maintained at 540 °C for growth. The Sb/Ga flux ratio was at least 3:1.

III. RESULTS AND DISCUSSION

A. MBE and RHEED

The surface reconstruction displayed a (1×3) diffraction pattern during growth. After MBE growth of about 500 Å of GaSb, the Ga flux was shut off and the sample cooled to ~200 °C under an Sb flux. As the sample cooled, the $\frac{1}{3}$- and $\frac{2}{3}$-order diffraction spots elongated and moved closer together, and a $c(2\times10)$ pattern emerged. The $\frac{1}{5}$- and $\frac{4}{5}$-order spots of the $c(2\times10)$ initially were very weak, but became more intense as the sample cooled further. After the $c(2\times10)$ was fully established, the Sb flux was terminated and the sample was annealed at 200 °C for 10 min and then allowed to cool to room temperature (RT). The RHEED pattern at RT showed a high-quality $c(2\times10)$, with the $\frac{1}{5}$- and $\frac{4}{5}$-order spots somewhat weaker than the $\frac{2}{5}$- and $\frac{3}{5}$-order spots. A photograph of the $c(2\times10)$ RHEED pattern is shown in Fig. 1(a). This surface is definitely Sb rich by the nature of the preparation procedure. This $c(2\times10)$ surface is stable up to about 375 °C, beyond which it undergoes an irreversible transformation to a $c(2\times6)$.

The $c(2\times6)$ surface can be generated by terminating the surface with an Sb flux at 400–450 °C after MBE,[1,2] but the highest-quality $c(2\times6)$ pattern was obtained by annealing the $c(2\times10)$ surface for 10 min at 440 °C. Figure 1(b) shows the $c(2\times6)$ RHEED pattern. The centered $\frac{1}{2}$-order spots are very bright and pointlike, indicating good long-range order.

Annealing the $c(2\times6)$ for 10 min at 500 °C caused the $\frac{1}{2}$-order dots to become faint, elongated streaks. Annealing for another 10 min at 530 °C caused them to fade markedly, giving what appears to be a $(1\times3)/c(2\times6)$ diffraction pattern with very faint centered $\frac{1}{2}$-order streaks, as shown in Fig. 1(c). The (1×3) RHEED is of poorer quality and has higher background than the $c(2\times6)$, indicating the presence of some surface disorder.

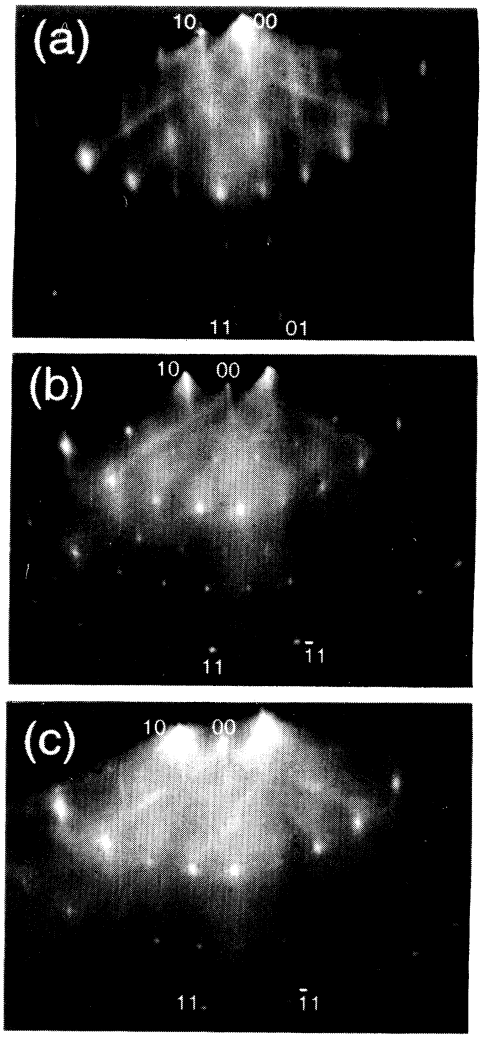

FIG. 1. RHEED photographs of (a) $c(2\times10)$, (b) $c(2\times6)$, and (c) (1×3) reconstructions. Some of the major diffraction spots are labeled.

RHEED of the (1×3) surface prepared by sputtering and annealing alone (without MBE) yielded similar patterns.

We have also observed a faint $c(4\times4)$ or $c(4\times12)$ periodicity coexistent with the $c(2\times6)$ and (1×3). This pattern is strongest during the transition from the $c(2\times6)$ to the (1×3). Annealing the $c(2\times6)$ for 10 min at 460 °C caused the $c(4\times4)$ pattern to intensify, while the $\frac{1}{2}$-order streaks of the $c(2\times6)$ became fainter. We observed this $c(4\times4)$ reconstruction on several occasions, although samples which exhibited a poorer-quality $c(2\times6)$ failed to show this structure, possibly due to higher background washing out the faint streaks. Previous RHEED studies have also noted the presence of a faint $(4\times?)$ pattern.[6] However, overall the $c(4\times4)$ was much fainter than the $c(2\times6)$, and is not distinct, so we do not report further on this structure here.

B. Qualitative analysis of core-level spectra

Photoemission spectra of the Sb 4*d* and Ga 3*d* cores were obtained at photon energies from 50 to 125 eV. These spectra recorded both the Sb 4*d* and Ga 3*d* cores. The total area under the Sb and Ga core levels was extracted from the data and recorded as an Sb/Ga intensity ratio for each surface. The Sb/Ga ratios as a function of $h\nu$ for the $c(2\times10)$, $c(2\times6)$, and (1×3) surfaces are shown in Fig. 2. It is clear from these ratios that the $c(2\times10)$ is the most Sb rich of the reconstructions, followed by the $c(2\times6)$ and (1×3).

Information about the surface structure can be obtained by decomposing high-resolution Sb 4*d* and Ga 3*d* core-level spectra into surface and bulk components. The spectra were analyzed by fitting the experimental-data to a linear combination of Voight line shapes using standard methods. Table I gives the fitting parameters for the Sb and Ga cores for each of the reconstructions studied here. All fits assume the same Lorentzian width, Gaussian width, branching ratio, and spin-orbit splitting for bulk and surface-shifted components. We utilized the minimum number of components necessary to give a good fit.

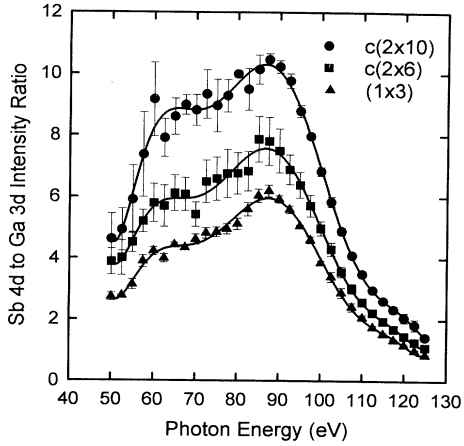

FIG. 2. Sb 4*d* to Ga 3*d* core-level intensity ratios for the three reconstructions. The curves are guides to the eye.

At the top of Fig. 3 is a representative Sb 4*d* core-level spectrum for the $c(2\times10)$ surface at a surface-sensitive photon energy. The spectrum exhibits a large surface-derived peak shifted 0.40 eV to higher binding energy, labeled $S1$. The $c(2\times10)$ core level appears upon inspec-

TABLE I. Line-shape parameters resulting from fits of the Sb 4*d* and Ga 3*d* core-level data for the various surfaces studied. All energies are in units of eV. Binding energies are referenced to the Fermi level. The branching ratio is the intensity ratio between the $j=\frac{3}{2}$ and $\frac{5}{2}$ spin-orbit split components. Lorentzian and Gaussian widths are the full widths at half maximum. Values quoted are averages for spectra obtained at many photon energies, except where specified.

	$c(2\times10)$	$c(2\times6)$	(1×3)
Sb:			
Lorentzian width	0.20[a]		
Spin-orbit splitting	1.249[a]		
Sb 3*d* binding energy	31.92	31.97	31.87
Branching ratio	0.67±0.03	0.67±0.02	0.68±0.01
Gaussian width	0.50±0.06	0.43±0.04	0.48±0.06
$S1/B@h\nu=72.5$ eV	1.40±0.05	0.84±0.02	0.42±0.05
$S1$ shift	−0.40±0.02	−0.422±0.007	−0.43±0.03
$S2/B@h\nu=72.5$ eV		0.54±0.04	0.42±0.02
$S2$ shift		0.45±0.02	0.43±0.02
Ga:			
Lorentzian width	0.20±0.04	0.28±0.05	0.28±0.05
Spin-orbit splitting	0.435[a]		
Ga 3*d* binding energy	19.00	19.07	18.90
Branching ratio	0.59±0.02	0.61±0.02	0.55±0.04
Gaussian width	0.37±0.03	0.32±0.04	0.30±0.04
$S1/B@h\nu=60$ eV			0.20±0.03
$S1$ shift			−0.49±0.03

[a]Values kept fixed for all fits.

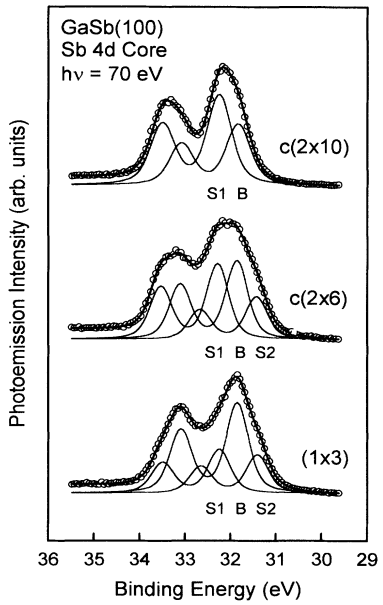

FIG. 3. Representative Sb 4*d* core-level spectra for each of the three reconstructions at a surface-sensitive photon energy of 70 eV. The bulk component is labeled *B*. *S*1 and *S*2 denote surface-shifted components. The data have been normalized to the peak maximum for display. Binding energies are referenced to the Fermi level.

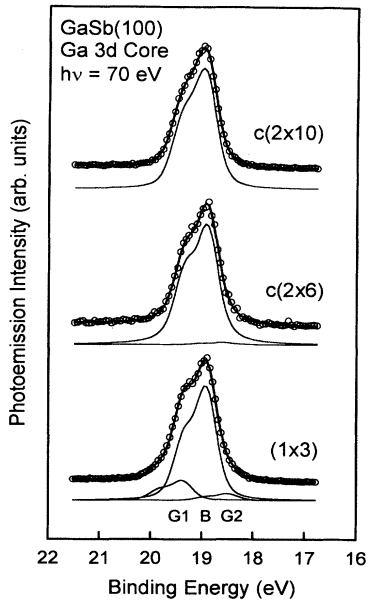

FIG. 4. Representative Ga 3*d* core-level spectra for each of the three reconstructions at a surface-sensitive photon energy of 70 eV. The (1×3) spectrum shows a surface-shifted component to higher binding energy labeled *G*1. The *G*2 peak is due to metallic Ga beads on the surface. The data have been normalized to the peak maximum for display. Binding energies are referenced to the Fermi level.

tion to be much like that of the InSb(100)-$c(4\times4)$ Sb 4*d* core level;[7] both have a large surface-shifted peak at higher binding energy, although the GaSb $c(2\times10)$ $S1/B$ ratio is about 1.5 times larger than the InSb $c(4\times4)$ S/B ratio: 1.5 vs 0.9 at the escape depth minimum. The InSb $c(4\times4)$ surface has been shown to be terminated by about $1-\frac{3}{4}$ ML of Sb.[7,8] It has been suggested that the surface shift to higher binding energy derives from group-V-to-group-V bonding. Since the $c(2\times10)$ is Sb rich, it seems reasonable that the *S*1 peak of the GaSb $c(2\times10)$ spectrum is due to Sb-Sb bonding, and might derive from more than $1-\frac{3}{4}$ ML of surface Sb.

The top spectrum of Fig. 4 shows the Ga 3*d* core for the $c(2\times10)$ surface. The core shows no obvious surface core-level shifts. Good fits were obtained with only one component, which is consistent with the absence of a surface Ga species for the $c(2\times10)$.

The middle spectrum of Fig. 3 shows a surface-sensitive Sb 4*d* core spectrum for the $c(2\times6)$ reconstruction. Two surface-shifted components are evident, labeled *S*1 and *S*2. The $S2/B$ ratio is about $\frac{2}{3}$ of the $S1/B$ ratio. This core spectrum appears similar to the GaAs(100)-$c(4\times4)$ As 3*d* core level,[9,10] with a large surface component to higher binding energy and a smaller component to lower binding energy. The sum of the $S1/B$ and $S2/B$ ratios at the escape depth minimum is about 1.4, equal to the $c(2\times10)$ $S1/B$ ratio of 1.4 (see Table I), indicating that the surface emission is due to similar amount of Sb for both surfaces.

The Ga 3*d* core for the $c(2\times6)$ (middle of Fig. 4) also gave good fits with the addition of a very small component (*G*2) to lower binding energy, which is due to the formation of small metallic Ga clusters as the surface is annealed.[1] Surfaces of III-V materials, after thermal annealing, often have an excess of group-III metals forming three-dimensional metallic clusters or beads on the surface. These clusters become larger for increased temperature or duration of the annealing. Spectra obtained on GaSb surfaces deliberately covered with Ga droplets by deposition show a similar component, which increases in intensity with increased Ga deposition. Apart from this metallic component, no obvious surface-shifted component is evident, however, which is consistent with the absence of a surface Ga species for the $c(2\times6)$ reconstruction.

The (1×3) Sb 4*d* core at the bottom of Fig. 3 is similar to those published by Ref. 1. The $S1/B$ ratio is about a factor of two smaller than the $c(2\times6)$ $S1/B$ ratio. The (1×3) $S2/B$ ratio is about the same as that for the $c(2\times6)$ surface. Both surfaces exhibit similar core-level shifts for each component. Spectra obtained from sputter-annealed surfaces exhibiting a (1×3) reconstruction are practically identical to those obtained by MBE and annealing. A previous study[1] determined that this surface is covered with 1–2/3 ML of Sb, with 1/3 ML of Ga atoms intermixed in the top layer. The *S*1 and *S*2 components of the Sb core were found to be due to about $\frac{2}{3}$ ML of Sb each, and our analysis (details follow)

concurs with this result. This surface may be related to the asymmetric (1×3) phase of InSb(100).[7,8] The Sb 4*d* cores of both surfaces appear similar, and the Ga 3*d* core of the GaSb(1×3) is very similar to the In 4*d* core of the InSb asymmetric (1×3). An STM study of the InSb asymmetric (1×3) supports the above model.[8]

The (1×3) Ga core at the bottom of Fig. 4 exhibits a tail on the high binding energy side, due to a surface-shifted component (labeled *G*1), which is absent in the *c*(2×6) spectra. This result indicates that a surface Ga species exists on the (1×3). The *G*2 component shifted to lower binding energy is more intense than that of the *c*(2×6), which is consistent with its assignation to metallic Ga. Annealing of the *c*(2×6) at higher temperatures to obtain the (1×3) surface would be expected to result in the formation of more Ga droplets. Prolonged annealing of the (1×3) surface at temperatures up to 600 °C and above, where substantial surface decomposition and formation of Ga droplets occur, produces no significant changes in the core level, except that the *G*2 metallic component increases.

There has been some question as to whether the *c*(2×6) and (1×3) surfaces are truly distinct surface phases, or are the same basic surface structure exhibiting varying amounts of disorder. Figure 5 shows the evolution of the Sb 4*d* *S*2/*B* and Ga 3*d* *G*1/*B* ratios as a function of surface annealing temperature. The dominant RHEED symmetry visible in the corresponding temperature range is noted above the upper axis. It is clear from the graph that there are three distinct surface phases. Shaded areas denote transition regions. The Sb *S*2/*B* ratio increases sharply at about 390 °C, and reaches a plateau at 410 °C, while the Ga *G*1 component does not appear until about 460 °C. These data coupled with the Sb/Ga ratios in Fig. 2 show conclusively that the *c*(2×6) and (1×3) are distinct surface phases. Although the weak *c*(2×6) streaks in the (1×3) RHEED hint at a possible admixture of *c*(2×6) and (1×3) regions, STM images of the (1×3) do not give any evidence for domain mixing.[1]

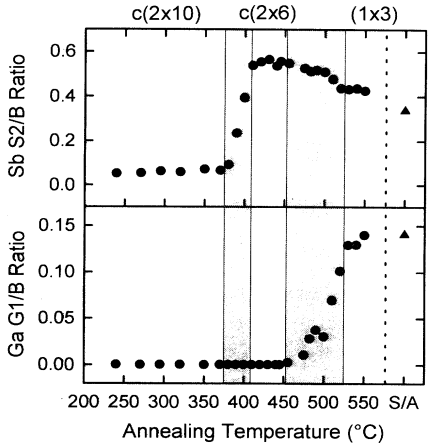

FIG. 5. Evolution of the Sb *S*2/*B* ratio and Ga *G*1/*B* ratio with annealing temperature. Three regions are evident. The RHEED symmetry visible in each region is noted above the top axis. Shaded areas represent transition regions. The *S*/*A* data points on the far right side of the graph, denoted by different symbols, were taken from a sputter/annealed surface exhibiting a (1×3) RHEED pattern.

From the above data, it is possible to posit simple models which qualitatively account for the observed *S*/*B* ratios and the Sb 4*d* to Ga 3*d* intensity ratios. Accepting the surface structure model of the (1×3) put forward by Refs. 1 and 6 implies that the *c*(2×6) is terminated by around $1-\frac{2}{3}$ ML of Sb with no surface Ga species, with the *S*2 component deriving from about $\frac{2}{3}$ ML and *S*1 from about 1 ML of Sb. Similarly, the *c*(2×10) is covered by more than 2 ML of Sb, with the surface-shifted emission due to about $1-\frac{2}{3}$ ML.

C. Quantitative analysis of Sb to Ga core intensity ratios

Standard layer-attenuation models will be utilized to place upper and lower bounds on the surface stoichiometry based on the measured Sb to Ga core-level intensities. Here we shall follow the method of John, Miller, and Chiang,[7] who used a similar analysis for InSb(100) surfaces. The major improvement in the present study is that a large number of data points measured over a wide photon energy range are included in the analysis. Oscillatory modulations of the intensity as a function of photon energy, due to photoelectron diffraction and interference effects, become evident. Only the average, smooth behavior is important for the layer attenuation analysis.

We will assume a base substrate, which is terminated by a full monolayer of Ga. The different models then assume that this base substrate is covered with varying amounts of Sb. The intensity ratio between the Sb and Ga core levels can be expressed as

$$\frac{I_{\mathrm{Sb}}}{I_{\mathrm{Ga}}}=\frac{\sigma_{\mathrm{Sb}}A_{\mathrm{Sb}}}{\sigma_{\mathrm{Ga}}A_{\mathrm{Ga}}}\ , \tag{1}$$

where σ_{Sb} and σ_{Ga} are the ML cross sections of Sb and Ga for photoelectron emission, respectively, and A_{Sb} and A_{Ga} are the corresponding photoelectron attenuation factors due to the finite escape depth in the solid. These attenuation factors for a GaSb surface covered with $\theta=n+x$ ML of Sb, with n an integer and $0<x<1$, are

$$A_{\mathrm{Sb}}(n,x,h\nu)=\frac{e^{-d/\lambda_s}+1-e^{-nd/\lambda_s}(1-x+xe^{-d/\lambda_s})}{1-e^{-2d/\lambda_s}}\ , \tag{2}$$

$$A_{\mathrm{Ga}}(n,x,h\nu)=\frac{e^{-nd/\lambda_g}}{1-e^{-2d/\lambda_g}}(1-x+xe^{-d/\lambda_g})\ , \tag{3}$$

where $d=1.53$ Å is the spacing between atomic planes, and λ_s, λ_g are the escape depths for Sb and Ga photoelectrons, respectively. We will use throughout this paper an escape depth of the form

$$\lambda(E,a,b)=\frac{a}{E^2}+b\sqrt{E}\ , \tag{4}$$

a common functional form used in analysis of photoemission and Auger data.[5,11,12] In Eq. (4), E is the photoelectron kinetic energy, which at a given $h\nu$ is different for Sb and Ga photoelectrons. For this analysis, we have chosen values of a and b yielding an escape depth minimum in the range of 4–6 Å at $E \cong 30$ eV. Experimental studies of the photoelectron escape depth in GaSb(110),[13] GaAs(110),[5,13] GaP(110),[4] and InSb(110) (Ref. 15) all give values for the escape depth minimum in the range of 4–6 Å. This broad range of a and b is chosen to take into account possible uncertainties due to diffraction effects.

Individual measurements of the Sb/Ga intensity ratio on a particular surface are not indicative of the atomic ratios of Sb to Ga, because the photoelectron cross sections σ_{Sb} and σ_{Ga} are not known. However, the *ratio* of Eq. (1) between two surfaces, say the $c(2\times10)$ and $c(2\times6)$, with coverages θ_1 and θ_2, respectively, is independent of the cross sections and depends only upon the coverages $\theta_1 = n_1 + x_1$ and $\theta_2 = n_2 + x_2$.

$$\left.\frac{\frac{I_{Sb}}{I_{Ga}}\Big|_{c(2\times10)}}{\frac{I_{Sb}}{I_{Ga}}\Big|_{c(2\times6)}}\right. \equiv R(h\nu) = \frac{A_{Sb}(n_1,x_1,h\nu)}{A_{Ga}(n_1,x_1,h\nu)} \frac{A_{Ga}(n_2,x_2,h\nu)}{A_{Sb}(n_2,x_2,h\nu)} . \tag{5}$$

Figure 6 shows the experimental measurements of $R(h\nu)$ for the $c(2\times10)/c(2\times6)$ and $c(2\times10)/(1\times3)$ surface pairs, along with model curves to be discussed later. Error bars denote the standard error from measurements taken on several different surfaces. The data show oscillatory modulations due to diffraction or interference effects, which should be ignored in the analysis based on the layer attenuation model. For each choice of θ_1, there exists a range of θ_2 values which satisfies the experimental data, due to the 4–6-Å escape depth range. The result of the analysis is summarized by the pair of diagonal lines shown in Fig. 7. These curves represent the upper and lower bounds on the $c(2\times10)$ coverage as a function of the $c(2\times6)$ coverage implied from our data. The actual coverages of the two surfaces must fall between the two curves. The y intercepts of these curves indicate that the $c(2\times10)$ has around 0.6–1.0 ML more Sb than the $c(2\times6)$.

It is possible to further restrict the range of possible $c(2\times10)$ and $c(2\times6)$ coverages by comparing absolute Sb and Ga core-level intensities between the two surfaces,[7]

$$\frac{I_{Sb}|_{c(2\times10)}}{I_{Sb}|_{c(2\times6)}} \equiv S = \frac{A_{Sb}(\theta_1,h\nu)}{A_{Sb}(\theta_2,h\nu)} ; \tag{6}$$

$$\frac{I_{Ga}|_{c(2\times10)}}{I_{Ga}|_{c(2\times6)}} \equiv G = \frac{A_{Ga}(\theta_1,h\nu)}{A_{Ga}(\theta_2,h\nu)} . \tag{7}$$

Equations (6) and (7) can be used to eliminate θ_2, giving $\theta_1(S,G,h\nu)$ and, eliminating θ_1, $\theta_2(S,G,h\nu)$. S is measured to be 1.11 and G is measured to be 0.80 (averaged over $h\nu = 50$–125 eV). With the same restrictions on λ as above, the values for θ_1 and θ_2 fall within the rectangle in the center of Fig. 7. Since the surface Sb coverages must fall within the pair of diagonal lines and inside the box, these data suggest that the $c(2\times10)$ has 2–2.8 ML and the $c(2\times6)$ has 1.4–2 ML of Sb on the surface. A similar analysis of $c(2\times10)$ and (1×3) surfaces gives results consistent with the surface structure model of (1×3) put forward by Ref. 1 and a $c(2\times10)$ coverage of 2.1–3 ML.

Based upon the preceding analysis, structure models with 2–3 ML of surface Sb on the $c(2\times10)$, and 1–2 ML of Sb on the $c(2\times6)$ are consistent with the data. Since roughly the same number of atoms are contributing to the surface emission in the $c(2\times10)$ and $c(2\times6)$ Sb $4d$ cores, this implies that roughly a monolayer of Sb on the

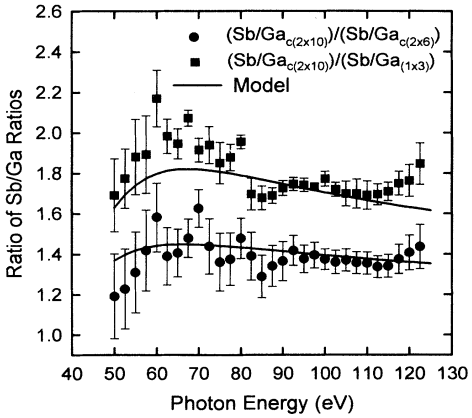

FIG. 6. The ratio of Sb/Ga intensity ratios for the $c(2\times10)/c(2\times6)$ and $c(2\times10)/(1\times3)$ pairs. The curves are model fits as described in the text.

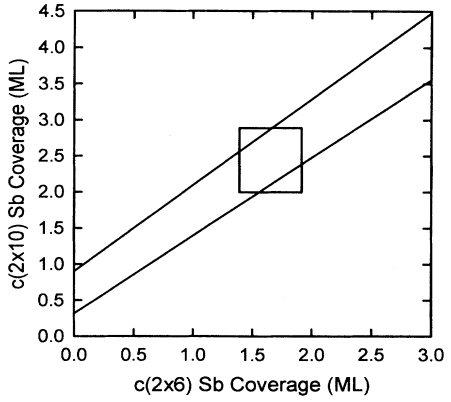

FIG. 7. The diagonal lines give the upper and lower bounds of $c(2\times10)$ surface Sb coverage as a function of $c(2\times6)$ surface Sb coverage as determined from analysis of the Sb/Ga ratios. Analysis of the relative intensities of Sb $4d$ core levels places the surface Sb coverages somewhere within the boxed-in area.

$c(2\times10)$ does not exhibit a core-level shift (coincident with the bulk emission).

D. Quantitative analysis of surface-to-bulk intensity ratios

Figures 8–10 show the photon energy dependence of the Sb $4d$ S/B ratios for each of the three reconstructions. As before, error bars denote the standard error from measurements taken on several different surfaces. The overall trend of the data reflects the change in the photoelectron escape depth with kinetic energy: the S/B ratio is the largest at the escape depth minimum near ~30-eV kinetic energy. However, it is evident that these curves are not smooth functions of photon energy. Oscillatory modulations due to diffraction and interference effects are very noticeable.

More detailed information about the surface structures can be obtained by a quantitative analysis of the S/B ratios. As mentioned in the Introduction, the traditional approach has been to apply the layer-attenuation model to S/B data obtained at one photon energy near the escape depth minimum. However, due to uncertainties caused by the diffraction and interference effects, it is really necessary to examine a range of photon energies. In our analysis, we have chosen to compare the measured values of the S/B intensity ratio as a function of incident photon energy to a "theoretical" S/B ratio curve calculated using the layer-attenuation model. Such model curves show the overall trend of the S/B ratio data, but will not reproduce the short-period EPFS oscillations. The only free parameters in this method are the escape depth constants a and b and the surface coverage. The model calculations must not only yield S/B ratios comparable to the data, but also Sb/Ga ratios consistent with measured values and an escape depth minimum in the range of 4–6 Å. In other words, data presented in Figs. 6 and 8–10 are taken into account simultaneously in a global fit. Many different combinations of surface structure models were attempted. The parameters which gave the best fit are summarized in Table II. The best fit was obtained with an escape depth minimum of 5.6 Å. The following paragraphs discuss each of the three reconstructions.

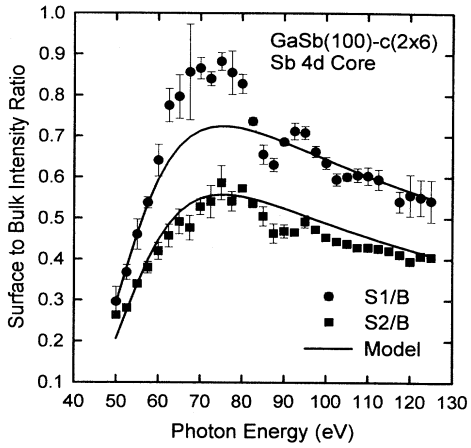

FIG. 9. The photon energy dependence of the $S1/B$ and $S2/B$ ratios for the $c(2\times6)$ reconstruction. The curves are model fits as described in the text.

1. The (1×3) surface

Figure 8 shows the photon energy dependence of the Sb $4d$ $S1/B$ and $S2/B$ ratios. Strong oscillations are evident in both ratios, particularly around 90 eV. The best model fit to the data was obtained by assuming that the (1×3) has a full monolayer of Sb with a fraction x ML of Sb and $(1-x)$ ML of Ga atoms on top.[1,8] The $S1$ component was assumed to be due to the x ML of Sb atoms in the second layer. The other $(1-x)$ ML of Sb atoms in the second layer are in a bulk configuration, since they are bonded to four Ga atoms. $S2$ was assumed to derive from the x ML of surface Sb. This model reverses the assignment of $S1$ and $S2$ of Ref. 1, in which only one pho-

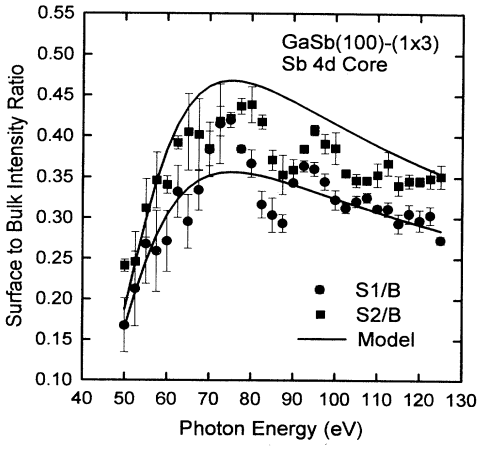

FIG. 8. The photon energy dependence of the $S1/B$ and $S2/B$ ratios for the (1×3) reconstruction. The curves are model fits as described in the text.

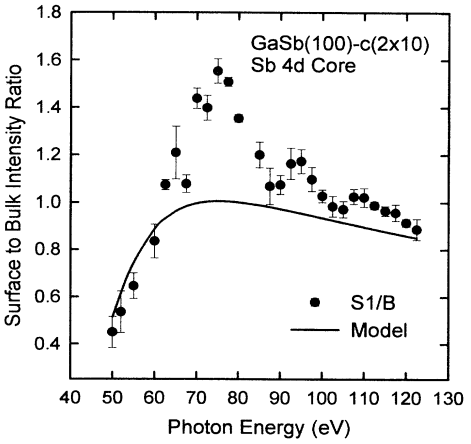

FIG. 10. The photon energy dependence of the $S1/B$ ratio for the $c(2\times10)$ reconstruction. The curve is a model fit as described in the text.

TABLE II. Best-fit parameters obtained from the data analysis.

Fit parameter	Best fit	Measured
a	1700	820–1375[a]
b	0.70	0.56–0.73[a]
$c(2\times10)$ Sb coverage (ML)	2.6	
$c(2\times6)$ Sb coverage (ML)	1.67	
(1×3) Sb coverage (ML)	1.63[b]	

[a]Values quoted from Ref. 5.
[b]Model used in fit implies 0.37 ML of Ga atoms on surface.

ton energy was used in the study. Our data show that while the $S1/B$ and $S2/B$ ratios are nearly the same and both correspond to about $\frac{2}{3}$ ML of Sb, the $S1/B$ ratio is slightly smaller, which would be expected from attenuation by the first-layer Sb above. The layer attenuation model then predicts

$$\left.\frac{S1}{B}\right|_{(1\times3)}=\frac{z(1-e^{-2d/\lambda})}{1-z+e^{-2d/\lambda}}\ ; \tag{8}$$

$$\left.\frac{S2}{B}\right|_{(1\times3)}=\frac{z(1-e^{-2d/\lambda})}{e^{-d/\lambda}(1-z+ze^{-2d/\lambda})}\ . \tag{9}$$

The curves resulting from this model are plotted in Fig. 8. The model gave the best fit with $x=0.63$, which is consistent with 2/3 ML of Sb and 1/3 ML of Ga on top of a full monolayer of Sb. The agreement with the $S1/B$ ratio is excellent, while the predicted $S2/B$ ratio is a bit high, possibly due to missing dimer defects or partial disorder on our samples. The RHEED pattern of this surface was of lower quality as noted above. Attempts were made to fit the data with other models, akin to the currently favored structures of the GaAs(100) and InSb(100)-$c(8\times2)$ reconstructions, but these models could not reproduce both the S/B ratios and Sb/Ga ratios.

2. The $c(2\times6)$ surface

For our model, we assumed that the $c(2\times6)$ was terminated by $(1+y)$ ML of Sb, as suggested by the analysis of Secs. B and C. The $S1$ component was assumed to derive from the full monolayer of second-layer Sb, and the $S2$ component was assumed to derive from the y ML of surface atoms. The calculated S/B ratios are

$$\left.\frac{S1}{B}\right|_{c(2\times6)}=\frac{1-e^{-2d/\lambda}}{e^{-2d/\lambda}}\ ; \tag{10}$$

$$\left.\frac{S2}{B}\right|_{c(2\times6)}=\frac{y(1-e^{-2d/\lambda})}{(1-y)e^{-2d/\lambda}+ye^{-3d/\lambda}}\ . \tag{11}$$

Note that the $S1/B$ ratio is independent of the surface coverage y, and is dependent *only* upon the characteristics of the escape depth curve. The curves resulting from this model with $y=\frac{2}{3}$ are plotted in Fig. 9. The agreement is excellent for both S/B ratios. It is apparent from the comparison of the data and model for the $S1/B$ ratio that the data show an intense peak at the escape depth minimum (~75 eV photon energy) followed by a minimum and another smaller peak, etc. These are not predicted by the simple layer-attenuation model, and illustrate the errors that can be introduced by sampling the S/B ratio at only one arbitrarily chosen photon energy.

3. The $c(2\times10)$ surface

This surface shows only one surface component for the Sb core, and no surface Ga emission. Figure 10 shows the photon energy dependence of the $S1/B$ ratio for the Sb core. Our model assumes that this surface is covered by $(2+z)$ ML of Sb, as suggested by the analysis of Secs. B and C. Since the $S1/B$ data exhibit $h\nu$-dependent oscillatory modulations that are very similar to the $S1/B$ ratios for the $c(2\times6)$ and (1×3) surfaces, it is reasonable to assume that it derives from the same site, that is, subsurface Sb bonded under Sb. The $S1/B$ ratio for the $c(2\times10)$ is about twice that of the $c(2\times6)$; therefore, $S1$ is assumed to derive from the second and third layers of Sb only, with the top layer included in the bulk intensity. This model gives

$$\left.\frac{S1}{B}\right|_{c(2\times10)}=\frac{(xe^{-d/\lambda}+1)(1-e^{-2d/\lambda})}{(1-x)e^{-d/\lambda}+xe^{-2d/\lambda}}\ . \tag{12}$$

Calculations assuming that $S1$ is due to only the uppermost layer or all three layers of Sb did not give satisfactory results. The curve of Fig. 10 represents the $S1/B$ ratio obtained from $z=0.6$, or a surface Sb coverage of about 2.6 ML.

4. The Sb/Ga ratios

Figure 6 shows the experimental ratios of Sb/Ga ratios R for the three surfaces, as discussed earlier. The curves are the results of the models detailed above. The agreement is very good overall. Attempts to reduce the amount of surface Sb by 1 ML for all reconstructions could predict the Sb/Ga ratios well at a very short escape depth (around 3 Å), but failed to accurately predict the magnitude of the S/B ratios. It is worth emphasizing that the above models were the only ones found to satisfy all of the data.

5. The escape depth

Occasionally, an escape depth minimum as short as 2–3 Å can be found in the literature. But those reports were typically based on measurements using only one photon energy chosen to maximize the surface sensitivity, or the S/B intensity ratio. Our data displayed in Figs. 8–10 clearly show the importance of diffraction and interference effects, which can render the S/B ratio significantly larger than what is predicted by the layer-attenuation model. If one takes the maximum S/B ratio (at a peak of EPFS oscillations), and inverts it using the layer-attenuation model, a much shorter "escape depth" will be obtained, which can be quite misleading.

E. Structural models

Based on the above analysis, we can now propose structural models, as shown in Figs. 11–13. Figure 11 is the same as the model of Refs. 1 and 6 for the (1×3). Figure 12 shows our proposed $c(2\times6)$ structure, with $1-\frac{2}{3}$ ML of Sb on the surface. Parallel Sb dimer chains are separated by staggered dimers in the second layer. The antiphase ordering of these second-layer dimers forms the $c(2\times6)$ symmetry. The $c(2\times6)$ is very similar to the (1×3) structurally; the main difference is the absence of the 1/3 ML of surface Ga atoms in between the Sb dimer chains. The weak $\frac{1}{2}$-order features in the (1×3) RHEED could be due to lateral buckling of the Ga atom chains. The $c(2\times10)$ surface model, shown in Fig. 13 has 2.6 ML of Sb, with the top layer forming triple-dimer blocks similar to the GaAs(100)-$c(4\times4)$ and InSb(100)-$c(4\times4)$ surfaces. Staggering of these blocks gives rise to the centered reconstruction.

F. Valence bands

For completeness, we show valence-band spectra for the three reconstructions in Fig. 14. These spectra are surface sensitive, and differences are easily noticed. This is consistent with the very different surface stoichiometries noted above. All three surfaces exhibit little emission at the Fermi level, suggesting that the surfaces are nonmetallic.

IV. CONCLUSION

The major reconstructions of the GaSb(100) surface were investigated using RHEED and core-level photoemission spectroscopy. Quantum-mechanical diffraction effects have been shown to have a significant effect on the measured S/B intensity ratios. At a diffraction or interference maximum, the measured S/B ratio can be substantially higher than that predicted by the layer-

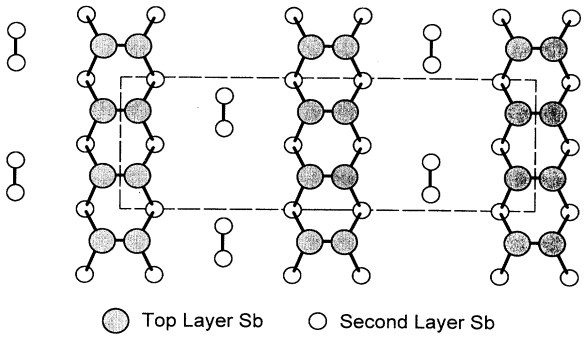

FIG. 12. Ball and stick model proposed for the $c(2\times6)$ surface with a Sb coverage of $1-\frac{2}{3}$ ML. Parallel Sb dimer rows are separated by second-layer dimers in an antiphase ordering, which gives the $c(2\times6)$ symmetry.

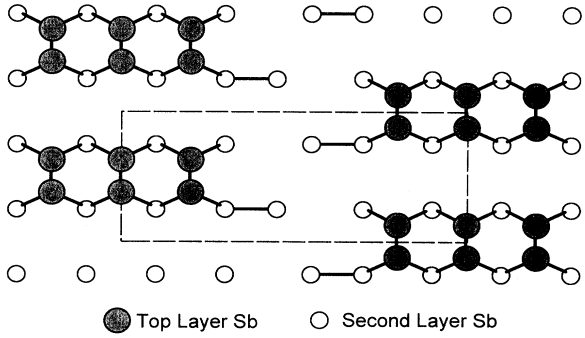

FIG. 13. Ball and stick model proposed for the $c(2\times10)$ surface. This model has a surface Sb coverage of 2.6 ML. A (2×5) unit cell is outlined. The antiphase ordering of the triple-dimer blocks results in the $c(2\times10)$ symmetry.

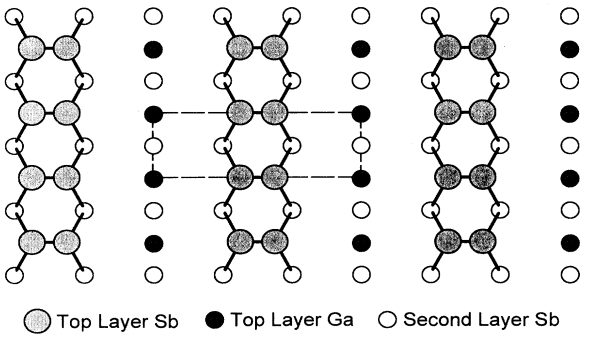

FIG. 11. Ball and stick model proposed for the (1×3) surface. This model has $1-\frac{2}{3}$ ML of Sb and $\frac{1}{3}$ ML of Ga on the surface. Parallel Sb dimer rows give rise to the strong $\times3$ symmetry observed with RHEED. Lateral buckling of the Ga chains could cause the weak $\times2$ features in the RHEED pattern, and contribute to surface disordering.

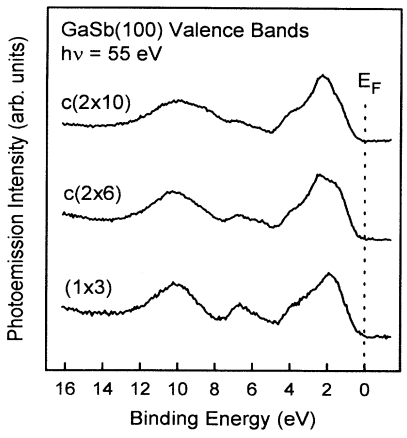

FIG. 14. Valence-band photoemission spectra for each of the three reconstructions. Binding energies are referenced to the Fermi level.

attenuation model, and care should be exercised in interpreting the results. Our analysis involving a wide range of photon energies overcomes these complications and gives a more accurate determination of surface stoichiometry from the analysis of core-level data than traditional methods. The escape depth minimum was found to be about 5.6 Å, which is in agreement with earlier measurements. The photoemission data strongly suggest that the $c(2\times10)$ surface is extremely Sb-rich, being terminated by more than 2 ML of Sb. It is surprising to find that the $c(2\times10)$ has so much surface Sb. However, there is some precedent for the existence of extremely Sb-rich InSb(100) surfaces, such as the InSb(100)-symmetric (1×3) or (1×1) reconstructions, both of which presumably have more than $1-\frac{3}{4}$ ML of Sb.[7] These surfaces perhaps could be described as Sb/GaSb and Sb/InSb adsorbate systems. Apparently there are no extremely group-V-rich (more than 2 ML) reconstructions for As or P based III-V(100) surfaces. Presumably this difference is related to the relative volatility of these three elements; P is the most volatile, while Sb is the least.

The $c(2\times6)$ and (1×3) are shown to be distinct surfaces phases, as evidenced by differences in their Ga/Sb ratios and surface core-level intensities. The $c(2\times6)$ is proposed to be covered by $1-\frac{2}{3}$ ML of Sb, with parallel dimer chains separated by second-layer Sb dimers, and is stoichiometrically similar to the GaAs(100)-$c(4\times4)$ and InSb(100)-$c(4\times4)$ surfaces. Our data support the structure model of the (1×3) surface put forward by previous studies, which has $1-\frac{2}{3}$ ML of Sb interdispersed with $\frac{1}{3}$ ML of Ga atoms. These models are fully consistent with our RHEED and photoemission observations.

ACKNOWLEDGMENTS

This material is based upon work supported by the Division of Materials Sciences, Office of Basic Energy Sciences, U.S. Department of Energy, under Grant No. DEFG02-91ER45439. An acknowledgment is also made to the Donors of the Petroleum Research Fund, administered by the American Chemical Society, and to the U.S. National Science Foundation (Grant No. DMR-92-23546) for partial support of the beam line operation and personnel. The Synchrotron Radiation Center of the University of Wisconsin is supported by the National Science Foundation.

[1]G. E. Franklin, D. H. Rich, A. Samsavar, E. S. Hirschorn, F. M. Leibsle, T. Miller, and T.-C. Chiang, Phys. Rev. B **41**, 12 619 (1990).
[2]T. H. Chiu and W. T. Tsang, J. Appl. Phys. **57**, 4572 (1985).
[3]C. E. C. Wood, K. Singer, T. Ohashi, L. R. Dawson, and A. J. Noreika, J. Appl. Phys. **54**, 2732 (1983).
[4]J. A. Carlisle, M. T. Sieger, T. Miller, and T.-C. Chiang, Phys. Rev. Lett. **71**, 2955 (1993).
[5]M. C. Schabel, I. M. Vitomirov, G. D. Waddill, and J. H. Weaver, J. Electron Spectrosc. Relat. Phenom. **56**, 211 (1991).
[6]J. R. Waterman, B. V. Shanabrook, and R. J. Wagner, J. Vac. Sci. Technol. B **10**, 895 (1992).
[7]P. John, T. Miller, and T.-C. Chiang, Phys. Rev. B **39**, 1730 (1989).
[8]C. F. McConville, T. S. Jones, F. M. Leibsle, S. V. Driver, T. C. Q. Noakes, M. O. Schweitzer, and N. V. Richardson, Phys. Rev. B **50**, 14 965 (1994).
[9]I. M. Vitomirov, A. Raisanen, A. C. Finnefrock, R. E. Viturro, L. J. Brillson, P. D. Kirchner, G. D. Pettit, and J. M. Woodall, Phys. Rev. B **46**, 13 293 (1992).
[10]M. T. Sieger, H. Farrell, and T.-C. Chiang (unpublished).
[11]M. P. Seah and W. A. Dench, Surf. Interface Anal. **1**, 1 (1979).
[12]H. Gant and W. Monch, Surf. Sci. **105**, 217 (1981).
[13]D. E. Eastman, T.-C. Chiang, P. Heimann, and F. J. Himpsel, Phys. Rev. Lett. **45**, 656 (1980).
[14]A. B. McLean and R. Ludeke, Phys. Rev. B **39**, 6223 (1989).
[15]V. Hinkel, L. Sorba, and K. Horn, Surf. Sci. **194**, 597 (1988).

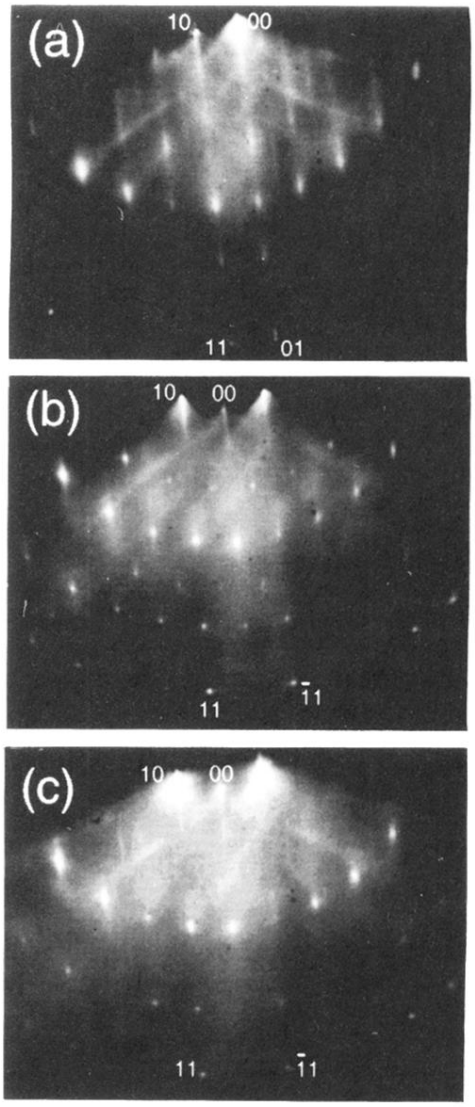

FIG. 1. RHEED photographs of (a) $c(2\times10)$, (b) $c(2\times6)$, and (c) (1×3) reconstructions. Some of the major diffraction spots are labeled.

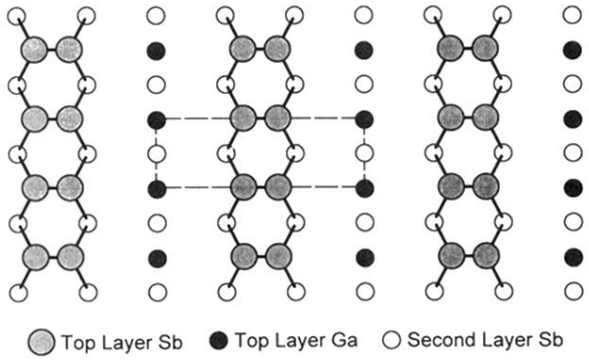

FIG. 11. Ball and stick model proposed for the (1×3) surface. This model has $1-\frac{2}{3}$ ML of Sb and $\frac{1}{3}$ ML of Ga on the surface. Parallel Sb dimer rows give rise to the strong $\times3$ symmetry observed with RHEED. Lateral buckling of the Ga chains could cause the weak $\times2$ features in the RHEED pattern, and contribute to surface disordering.

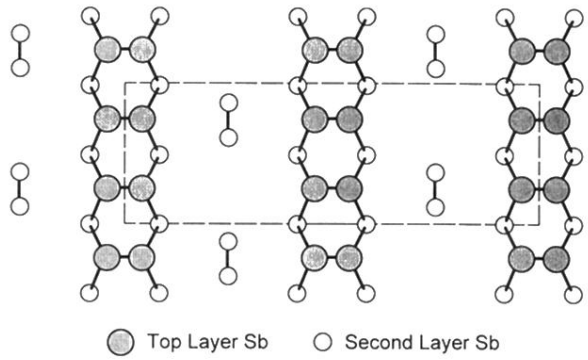

FIG. 12. Ball and stick model proposed for the $c(2\times6)$ surface with a Sb coverage of $1-\frac{2}{3}$ ML. Parallel Sb dimer rows are separated by second-layer dimers in an antiphase ordering, which gives the $c(2\times6)$ symmetry.

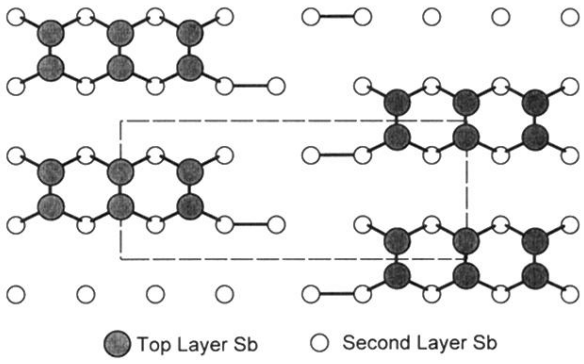

FIG. 13. Ball and stick model proposed for the $c(2\times10)$ surface. This model has a surface Sb coverage of 2.6 ML. A (2×5) unit cell is outlined. The antiphase ordering of the triple-dimer blocks results in the $c(2\times10)$ symmetry.

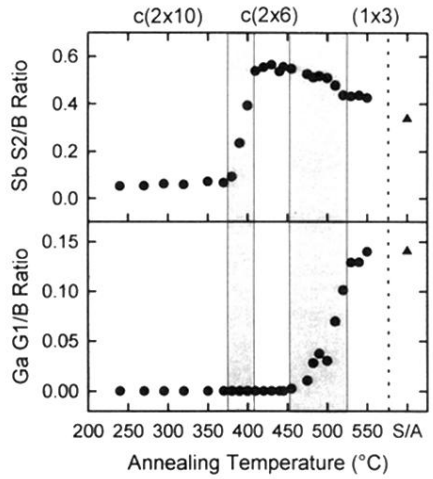

FIG. 5. Evolution of the Sb $S2/B$ ratio and Ga $G1/B$ ratio with annealing temperature. Three regions are evident. The RHEED symmetry visible in each region is noted above the top axis. Shaded areas represent transition regions. The S/A data points on the far right side of the graph, denoted by different symbols, were taken from a sputter/annealed surface exhibiting a (1×3) RHEED pattern.